

FPMC2018-8832

LOW SPEED PERFORMANCE OF AXIAL PISTON MACHINES

Peter Achten
INNAS
Breda, Netherlands

Jeroen Potma
INNAS
Breda, Netherlands

Jasper Achten
INNAS
Breda, Netherlands

ABSTRACT

Low speed operation of axial piston motors has always been a critical performance issue. The breakaway torque determines the capacity of a motor to move a certain load from standstill conditions. In addition, the low speed performance has also become a critical performance parameter for pumps being applied in frequency controlled electro-hydraulic actuators. Yet, there is almost no information available about the low speed and breakaway characteristics of piston pumps and motors.

A new test bench has been constructed to measure these characteristics [1]. The new bench allows operation of hydrostatic machines below 1 rpm, down to 0.009 rpm. At these conditions, the main tribological interfaces operate in the solid friction domain, at which the friction losses are at a maximum value.

This research describes and analysis the test results for a number of different axial piston pumps and motors: two slipper type motors, one slipper type pump and a floating cup pump/motor. The tests have been performed at various operating pressures and operating speeds. Furthermore, the breakaway torque has also been measured after letting the hydrostatic motor stand still for one or more days.

INTRODUCTION

The performance of hydrostatic motors at low operating speeds has always been an important criterion. Motors start at zero operating speeds, often in combination with a high load. Examples are wheel hub motors in forestry machines and motors for winch drives. When a forestry machine needs to climb up a slope, the torque losses of the motor at breakaway

conditions are added to the high gravitational load. The motors therefore need to be oversized in order to overcome these high initial friction losses. The friction also causes stick-slip effects and strong hysteresis in controlling speeds, for instance in winches, thereby reducing the productivity of cranes and other equipment.

As this paper will show, the rotational speed needs to be reduced to less than 1 rpm, in order enter into solid friction conditions and really measure the conditions at breakaway conditions. Testing of the behaviour of hydrostatic machines at such low rotational speeds is hardly investigated or reported in scientific publications. One of the first research works is published in 1991-1993 by Matsumoto and Ikeya [2-7]. In 1993, Maiti [8], investigated the torque losses at low rotational speeds of an epitrochoid generated rotary piston machine. This was followed in 1999 by another article from the same author and co-authored by M. Nagao [9], in which they investigated the starting torque characteristics of orbital hydraulic motors. Another study was reported by Dasgupta [10]. In 2004, the IFAS institute in Aachen tested a number of axial piston pumps, operated as a motor at 0.1 rpm [11]. Hong, et al [12-14], studied the effect of PVD-coatings of TiN on the startup friction behaviour of a bent axis motor. The tests were performed at relatively high operating speeds of 50 rpm. Lee, et al [15] investigated the friction of the slipper of a slipper type pump at low operating speeds, between 10 and 100 rpm. Another set of articles is published by Paul Michael, et al, from Milwaukee School of Engineering [16-18].

Recently the Dutch company INNAS has build a new test bench [1], in which a new type of low speed test bench was combined with, and integrated into a normal high speed test bench. The test bench allows operating speeds in a range between 0.009 and 5000 rpm. The maximum pressure level is

500 bar. This paper presents a number of tests performed on the new test bench.

SPECIFICATIONS OF THE PUMPS AND MOTORS

This paper reports about the test of four axial piston machines: two slipper type motors, one slipper type pump and a floating cup pump/motor. The geometrical displacement varies between 23.7 and 30.2 cc per revolution. The machines differ also in terms of maximum continuous pressure and maximum continuous speed:

Table 1: Specifications of the machines being tested

nr	type	displacement [cc]	maximum pressure [bar]	maximum speed [rpm]
1	slipper type motor	28,1	400	4250
2	slipper type pump	28,0	350	3750
3	slipper type motor	30,2	250	2000
4	floating cup pump/motor	23,7	500	5000

DESCRIPTION OF THE TEST BENCH AND TEST PROCEDURE

The test bench has been described in [1]. Figures 2 and 3 show the layout and the most important components. A simplified hydraulic circuit of the low speed part of the test bench can be found in Annex A.

At very low operating speeds, the leakage is larger than the effective flow which is created by the displacement. An additional pump is therefore needed to compensate for these losses (nr. 6 in Annex A). The rotational speed is defined by a linear actuator and a chain drive. The drive creates about two complete rotations of the test specimen. The angular position of the pump or motor is measured by means of the angular position sensor in the electric motor of the linear actuator. The linear actuator allows a near constant and repeatable definition of the rotational speed. The rotation can be in both directions, allowing all test objects to be tested as a pump and as a motor. The measurements can be extremely detailed. The measurement frequency is 5 kHz. For practical reasons, the measurements are also stored in a second file with a sample frequency of 50 Hz. For a measurement at 0.93 rpm, the latter file format results in about 9 measurement points per degree of rotation (3224 points for a single rotation). For a test at 0.12 rpm, this number is increased by a facto of 8, resulting in almost 26000 measurement points per 360° of rotation.

The normal test procedure starts with a performance test according to ISO4409:2007 [19]. This allows the oil and the test object to warm up. Subsequently, the geometrical displacement of the test object is determined in accordance with ISO8426:2008 [20]. After this, the low speed tests can be performed. This can be immediately following the high speed performance test i.e. at warm operating conditions. The advantage of the integrated test bench is that the test object can remain on the test bench, including all the sensors and

hydraulic lines. By means of shifting a coupling, the low speed test bench can be connected and activated. Due to this simple and fast procedure, it is possible to have a low speed test immediately following the high speed test. Aside from this, it is also possible to wait a certain amount of time, and measure the influence of a cold start. The paper will also present a result of such a test.

From the measured pressure difference Δp and the measured geometrical displacement, the maximum theoretical torque can be calculated:

$$M_{th} = \frac{\Delta p \cdot V_d}{2\pi} \quad (1)$$

Given this value, the torque loss ΔM can be calculated, subtracting the theoretical torque from the measured torque:

$$\Delta M = M_{meas} - M_{th} \quad (2)$$

The tests can be performed at various speeds, operating pressures and oil temperatures. The air content of the oil, i.e. the bulk modulus is controlled by means of an active system [21].

The new test bench allows a precise comparison of individual test runs. Figure 1 shows the repeatability of two separate tests of the same motor at the same operating conditions.

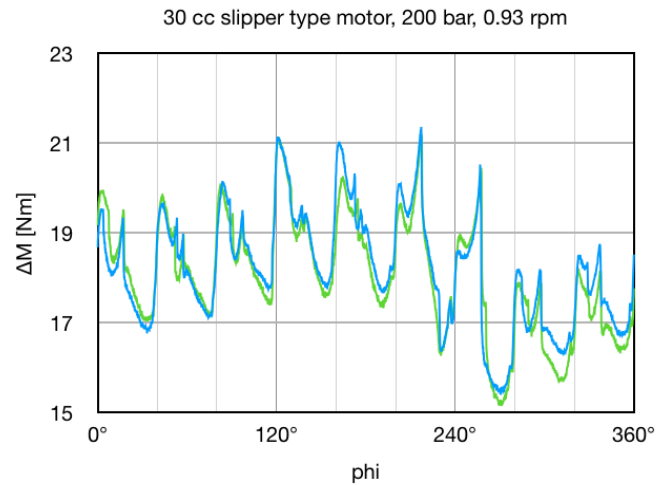


Fig. 1: Comparison of two different tests at equal test conditions

The test shows a significant variation of the torque loss. This is partly due to the limited number of pistons (in the above example there are 9 pistons). Furthermore, the variation is due to small differences in the tribological interfaces. Both the maximum torque loss and the average torque loss are derived from the measurements. In addition the oil temperature at the supply side, the return line and of the case drain flow are measured, as well as the case drain flow itself. A list of sensors can be found in Annex C.

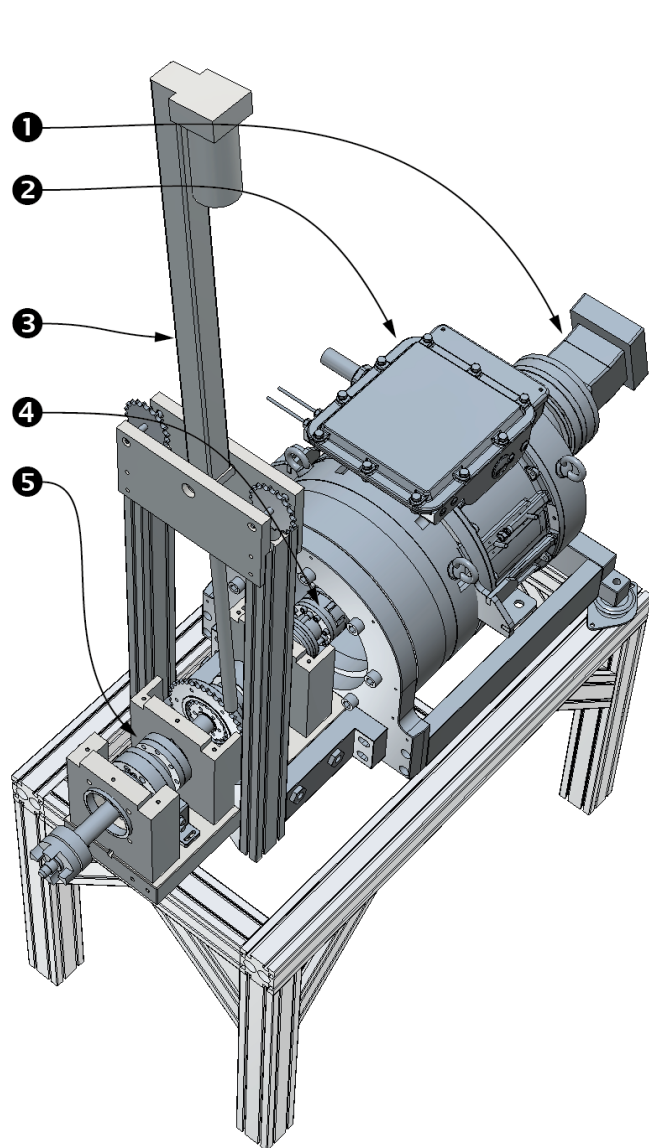


Fig. 2: INNAS combined test bed

1. Hydraulic motor or pump for power recirculation
2. Frequency controlled, water cooled electric motor
3. Linear electric actuator
4. Switchable coupling
5. Torque and speed sensor

MEASURED TORQUE LOSSES

The high speed performance measurements can be combined with the low speed measurements. By means of the measured geometrical displacement and the measured pressure difference, the torque losses can be derived for all test and operating conditions. Figure 4 shows the measured torque losses of the 4 test objects, at a pressure level of 200 bar. The oil temperature was 45°C (HLP46 oil).

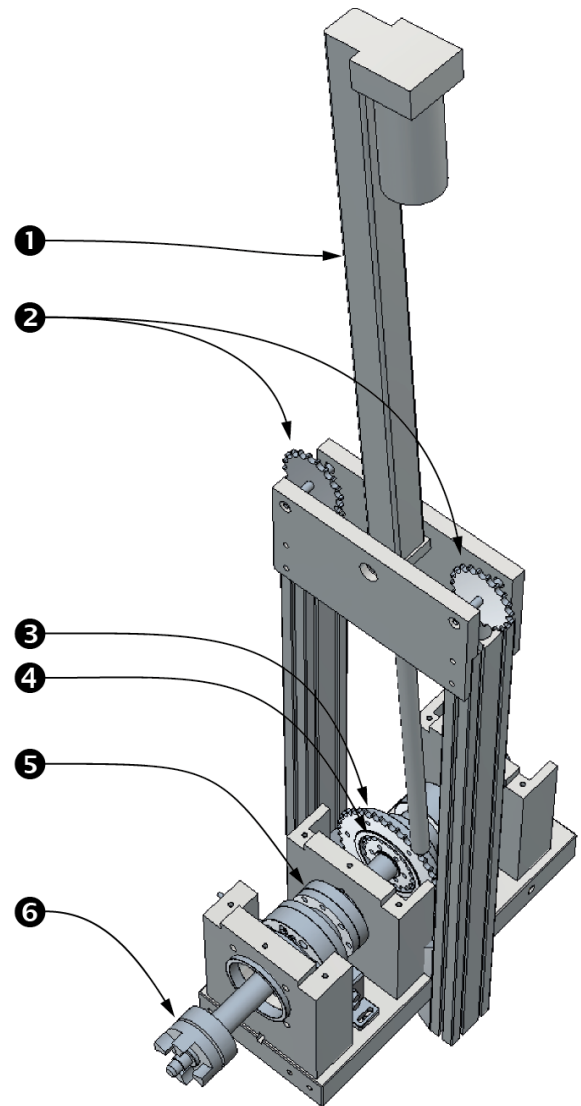


Fig. 3: Low-speed test bed
(the chain and counter weight are not shown)

1. Linear actuator with build-in position sensor
2. Sprockets for the counter weight, one for each direction of rotation
3. Sprocket with 60 teeth
4. Sprocket with 36 teeth
5. Torque sensor
6. Coupling for the pump or motor to be tested

At high operating speeds, all machines show a slight increase of the torque losses due to increased viscous friction of the hydrodynamical lubricated bearing interfaces. When being operated at lower rotational speeds, the bearing interfaces enter into the mixed lubrication regime, and, finally, in the solid friction domain. This can be seen clearer when the same graph is plotted as a log-log-diagram (Figures 5-8).

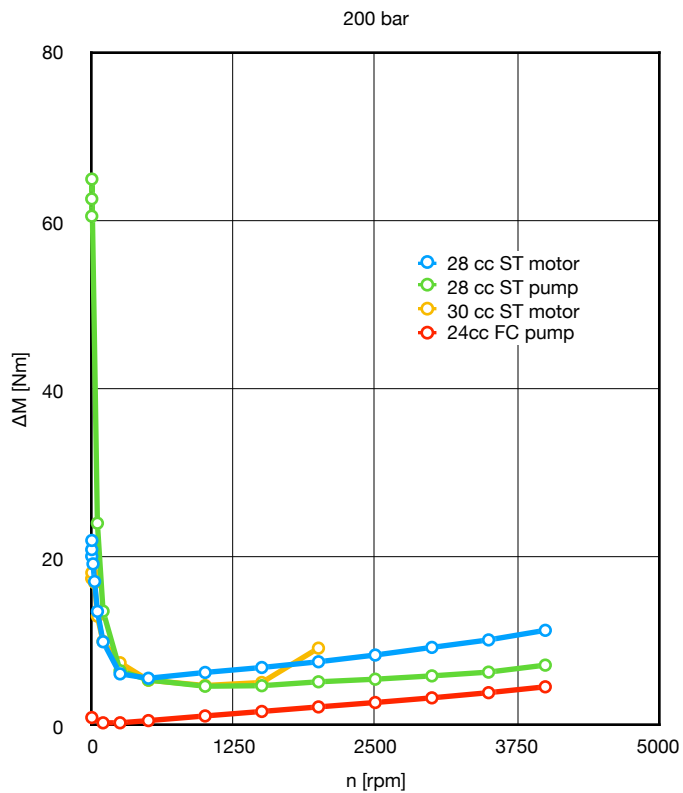


Fig. 4: Measured torque losses at 200 bar

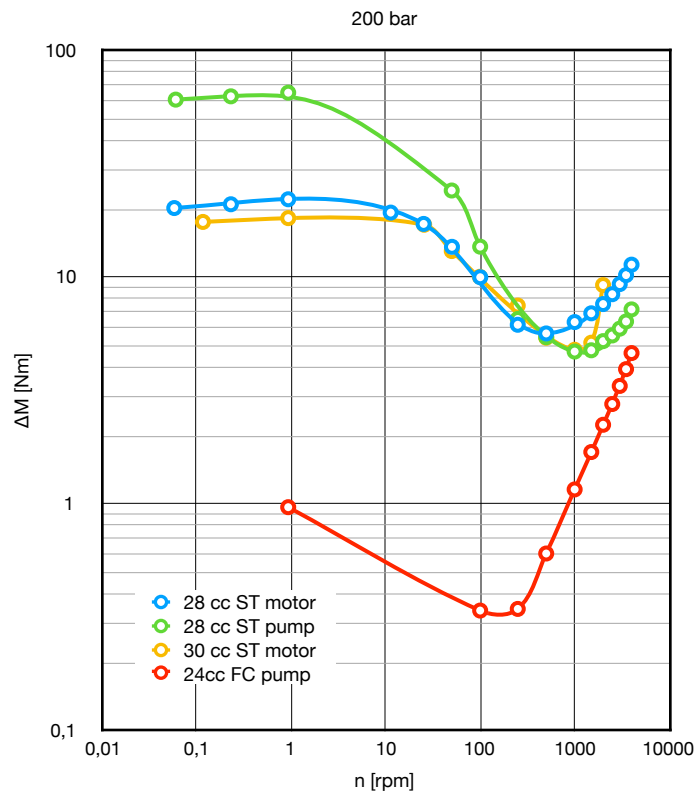


Fig.6: Measured torque losses at 200 bar

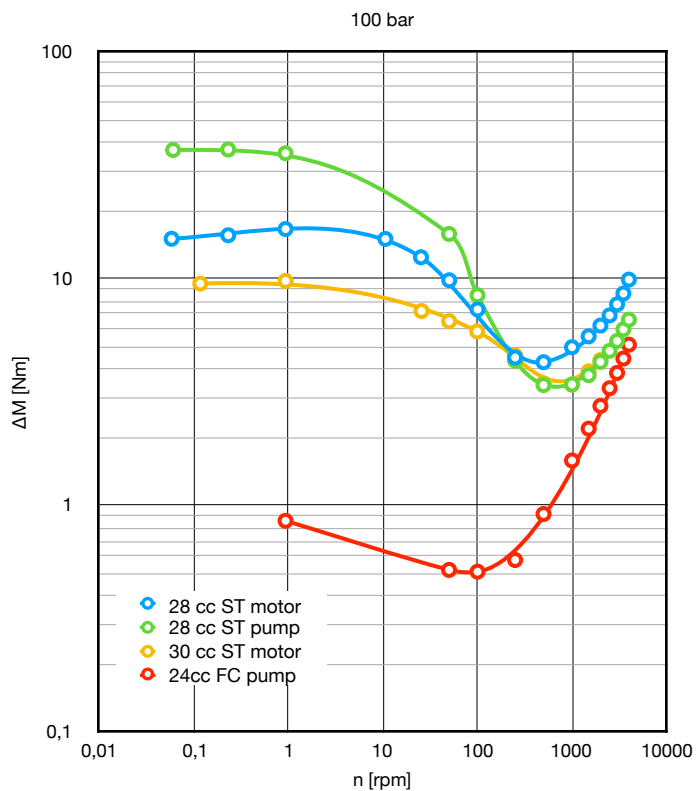


Fig.5: Measured torque losses at 100 bar

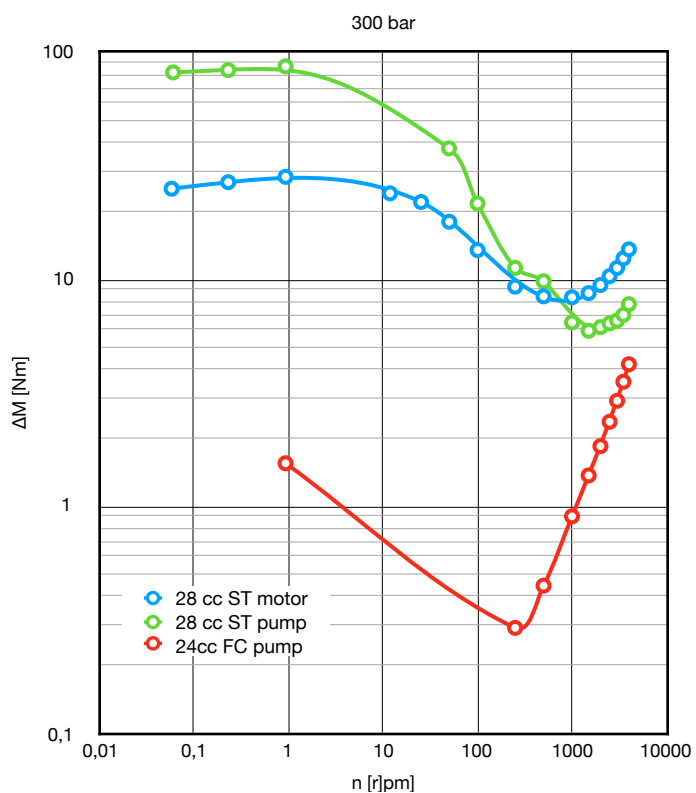


Fig. 7 Measured torque losses at 300 bar

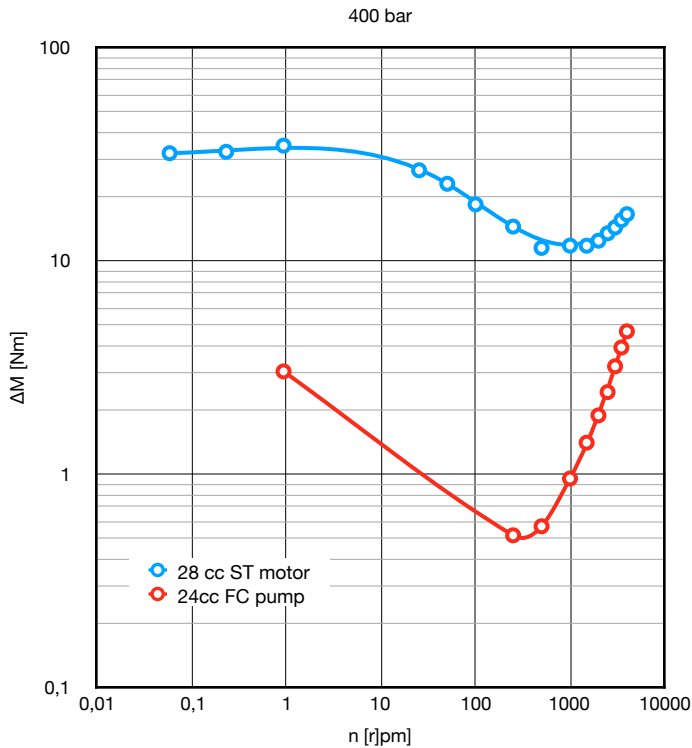


Fig. 8: Measured torque losses at 400 bar

Due to the maximum pressure limitations of the 30 cc motor, there are no test data for this motor at 300 and 400 bar. For the same reason there are also no test data for the 28 cc slipper type pump at a load of 400 bar. It should also be noted that the sizes slightly differ, which also influences the results. Compared to the 28 cc machines, the 30 cc is 8% bigger, and the 23.7 cc floating cup pump/motor is 15% smaller.

Nevertheless, the diagrams clearly show a difference between the three slipper type machines. The tests also show the much lower friction of the floating cup pump, especially at startup conditions and low operating speeds. The floating cup principle eliminates the friction between the pistons and the cylinders (or cups) [11]. In addition, the low barrel spring force [22] and the new hydrostatic bearing design of the barrel seal lands [23] further reduces the friction losses at low operating speeds. At high operating speeds, the friction losses are halved. At low operating speeds, the floating cup principle more than decimates the friction losses.

BREAKAWAY AFTER STANDSTILL

The friction conditions of the sliding bearing interfaces at near zero operating speeds depend on the amount of oil still being present in the gap. In order to verify this, tests have been performed after various standstill times of the test object. Figure 9 shows three low speed tests of the 28 cc slipper type motor. The first test was performed immediately following a warmup procedure. The other two tests were made after 1 day respectively 3 days of standstill, during which the oil and the motor cooled down to 19°C. Having the motor standing still for a day, the breakaway torque loss increases from about 25.7 Nm to 30.2 Nm, an increase of 18%. The third test, which was performed after three days waiting showed another increase of the torque loss to 33.1 Nm, 29% higher than at a warm start.

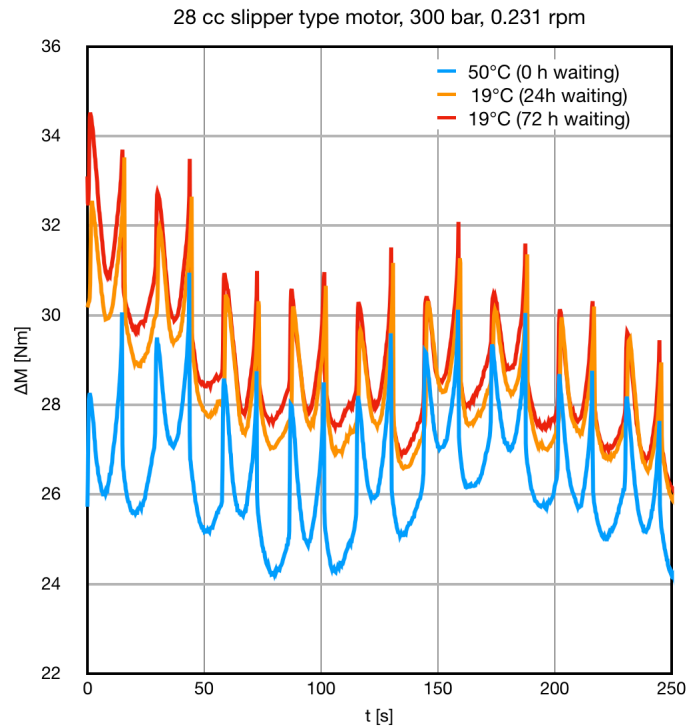


Fig. 9: Effect of standstill on the breakaway torque loss

PUMP AND MOTOR OPERATION

During low speed testing, the linear actuator makes a down stroke followed by a stroke in the upward direction. The test object is thereby tested first as a motor, followed by a test at pumping conditions. The following three diagrams compare the measured torque, the torque losses and the hydraulic-mechanical efficiencies of the 28 cc slipper type motor and the 24 cc floating cup pump/motor, while being operated as a pump and as a motor. The measurements have been performed at four different pressure levels. The rotational speed was 0.93 rpm. The results are shown in figures 10-12.

The floating cup pump/motor clearly performs better. During motor operation, the 23.7 cc floating cup motor outperforms the larger 28.2 cc slipper type motor.

The biggest difference is however during pump operation. The slipper type machine has a hydraulic-mechanical efficiency of 55% - 63%. This is for instance an important disadvantage for electro-hydraulic actuators when manoeuvring and control the speed and position of a hydraulic cylinder. In order to overcome the strong friction losses, the electric motor needs to be oversized by as much as 59%. The slipper type machine has an asymmetric behaviour, having much higher friction losses at pump operation than at motor operation. The floating cup machine doesn't show this difference in behaviour. The friction losses are extremely low during both motor operation and pump operation.

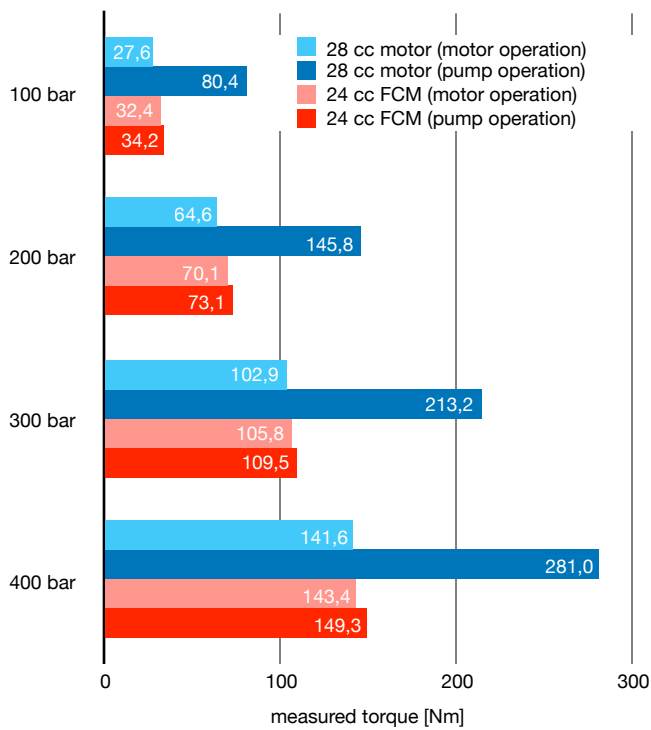


Fig. 10: Comparison of the measured torque during pump and motor operation of the 28 cc slipper type motor and the 24 cc floating cup pump/motor ($n = 0.93$ rpm)

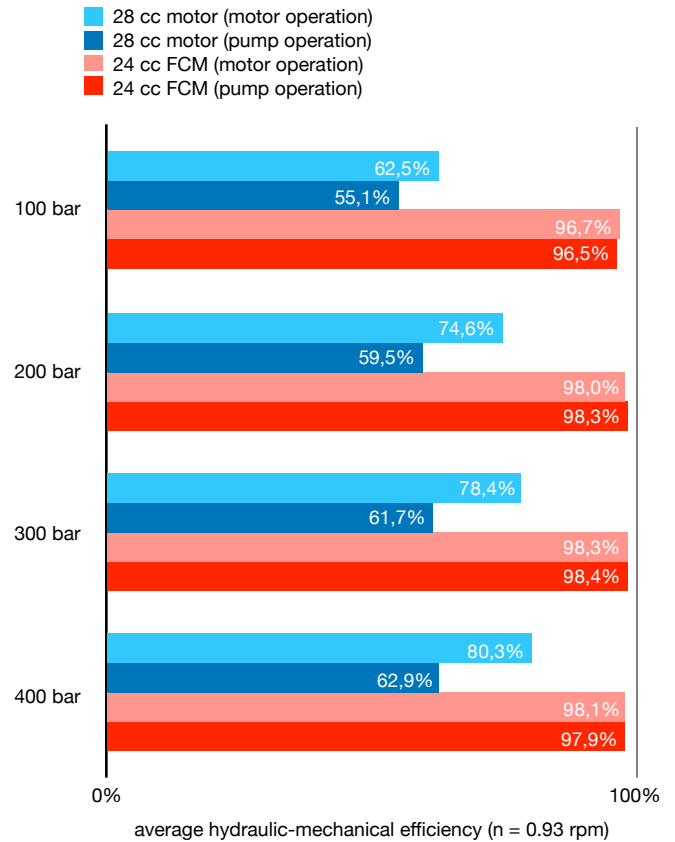


Fig. 12: Average hydraulic-mechanical efficiency at a rotational speed of $n = 0.93$ rpm

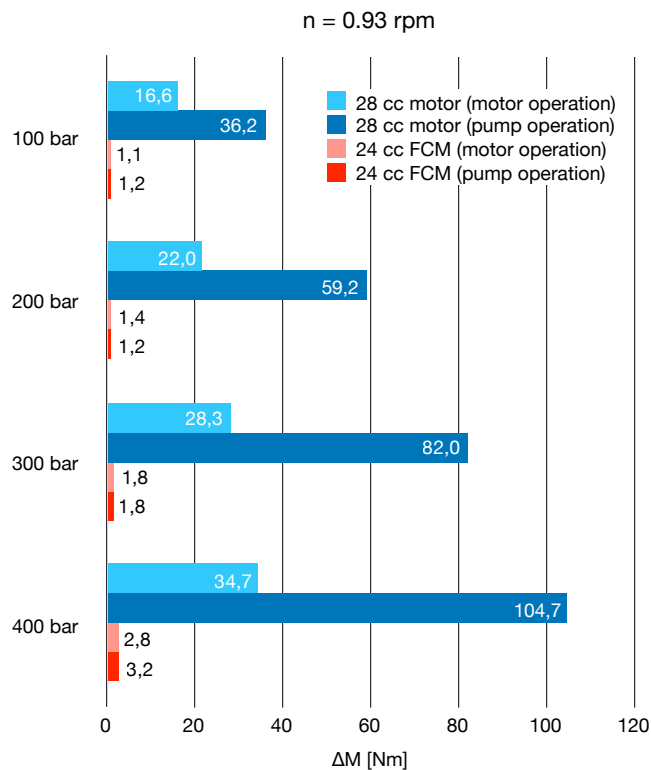


Fig. 11: Comparison of the average torque losses during pump and motor operation of the 28 cc slipper type motor and the 24 cc floating cup pump/motor ($n = 0.93$ rpm)

CONCLUSIONS

The new test bench integrates two test benches: one for high speeds up to 5000 rpm and one for low rotational speeds, down to 0.09 rpm. Four different axial piston pumps and motors have been tested at various operating pressures and rotational speeds.

The test results show significant differences between the pumps and motors being tested. The floating cup principle has the lowest friction losses: at low operating speeds and startup conditions, the friction losses are decimated compared to the slipper type machines.

The results from the test also clearly show the high friction losses from the slipper type pump compared to the slipper type motor. At high loads, the friction losses are three times higher as during motor operation. Compared to the floating cup pump, the friction losses are 30 to 48 times higher.

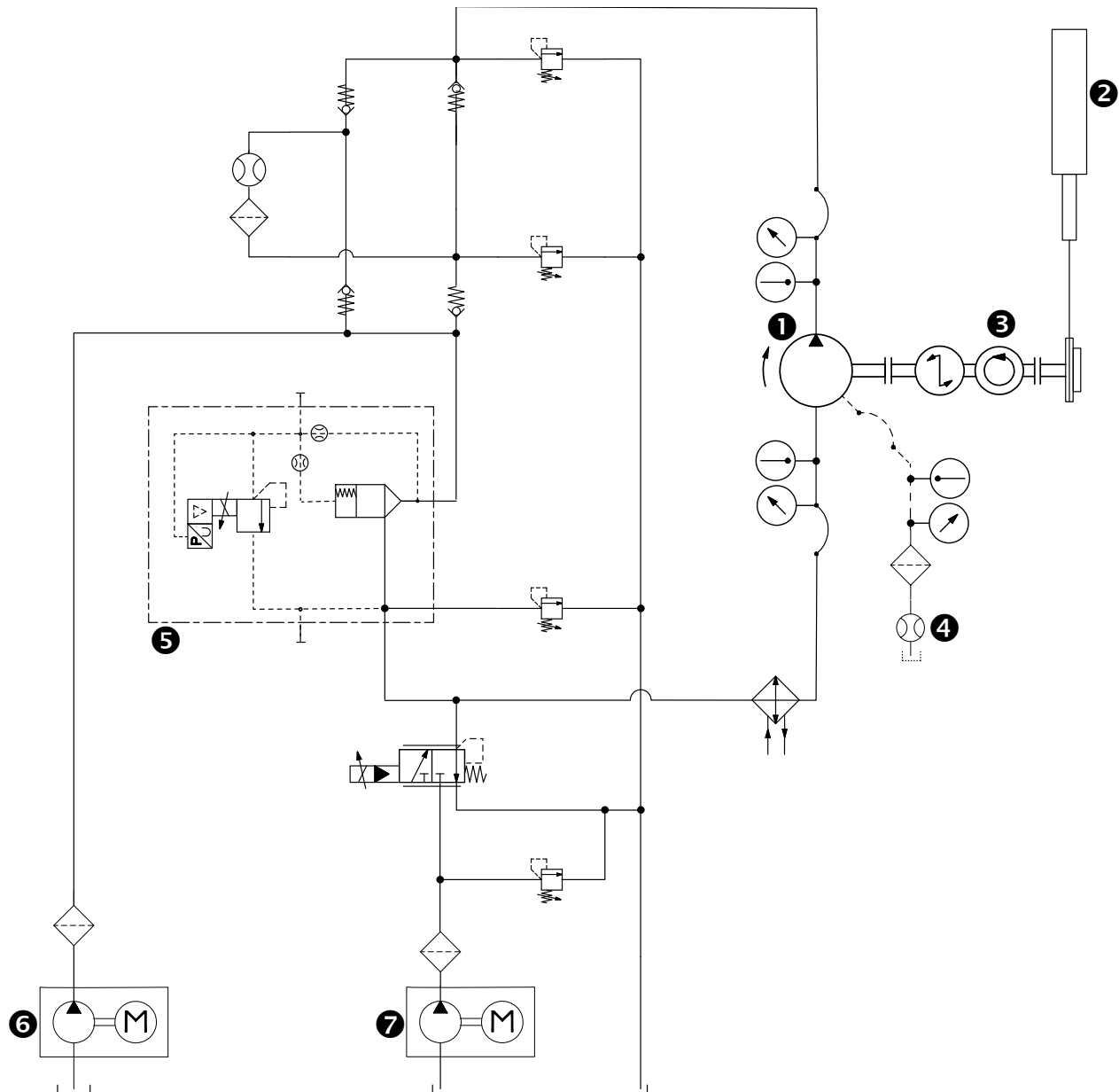
Finally, the measurements also show the influence of a standstill on the breakaway torque of the 28 cc slipper type motor. After one day waiting, the friction was 18% higher. After three days the losses were increased by as much as 29% compared to an immediate warm start after a standstill.

BIBLIOGRAFIE

1. Achten, P., J. Potma, and S. Eggenkamp. A New Hydraulic Pump and Motor Test Bench for Extremely Low Operating Speeds. in ASME/BATH 2017 Symposium on Fluid Power and Motion Control. 2017. Sarasota, Florida, USA.
2. Matsumoto, K. and M. Ikeya, Leakage Characteristics between the valve plate and cylinder for low-speed conditions in a swashplate-type axial piston motor. Transactions of the Japan Society of Mechanical Engineers Series C, 1991. 57(541): p. 3008-3012.
3. Matsumoto, K. and M. Ikeya, Friction Characteristics between the Piston and Cylinder for Low-Speed Conditions in a Swashplate-Type Axial Piston Motor. Transactions of the Japan Society of Mechanical Engineers Series C, 1991. 57(540): p. 2729-2733.
4. Matsumoto, K. and M. Ikeya, Friction Characteristics for Starting and Low-Speed Conditions of a Ball Joint in a Swashplate-Type Axial Piston Motor. Transactions of the Japan Society of Mechanical Engineers Series C, 1991. 57(538): p. 2017-2022.
5. Matsumoto, K. and M. Ikeya, Friction and Leakage Characteristics between the Slipper and Swashplate for Starting and Low-Speed Conditions in a Swashplate-Type Axial Piston Motor. Transactions of the Japan Society of Mechanical Engineers Series C, 1991. 57(541): p. 3013-3018.
6. Matsumoto, K. and M. Ikeya, Friction and Leakage Characteristics between the Valve Plate and Cylinder for Starting and Low-Speed Conditions in a Swashplate-Type Axial Piston Motor. Transactions of the Japan Society of Mechanical Engineers Series C, 1991. 57(538): p. 2023-2028.
7. Yi, F., K. Matsumoto, and M. Ikeya, Experimental Analysis of Leakage Characteristics for Starting and Low-Speed Conditions of Hydrostatic Slipper Bearing in Swashplate Type Axial Piston Motor. Hydraulics & Pneumatics, 1992. 23(1): p. 107-112.
8. Maiti, R., Torque characteristics of epitrochoid generated orbital rotary piston type hydraulic motors. Mechanism and Machine Theory, 1993. 28(2): p. 225-231.
9. Maiti, R. and M. Nagao, Prediction of starting torque characteristics of epitrochoid generated orbital rotary piston hydraulic motors. JSME International Journal. Series C: Mechanical Systems, Machine Elements and Manufacturing, 1999. 42(2): p. 416-426.
10. Dasgupta, K., Analysis of a hydrostatic transmission system using low speed high torque motor. Mechanism and Machine Theory, 2000. 35(10): p. 1481-1499.
11. Achten, P., et al., Efficiency and Low Speed Behavior of the Floating Cup Pump, SAE 2004-01-2653. 2004.
12. Hong, Y.-S., et al., Improvement of the low-speed friction characteristics of a hydraulic pump by PVD-coating of TiN. Journal of Science and Technology (KSME Int. J.), 2006. 20(3): p. 358-365.
13. Lee, S.-Y. and Y.-S. Hong, Effect of CrSiN thin film coating on the improvement of the low-speed torque efficiency of a hydraulic piston pump. Surface & Coatings Technology, 2007. 202: p. 1129-1134.
14. Hong, Y.-S. and S.-Y. Lee, A Comparative Study of Cr-X-N (X=Zr, Si) Coatings for the Improvement of the Low-Speed Torque Efficiency of a Hydraulic Piston Pump. Metals and Materials International, Vol. 14, No. 1 (2008), pp. 33-40, 2008. 14(1): p. 33-40.
15. Lee, S.L., et al., Investigation of the Tribological Effects of the Auxiliary Inner Ring for Piston Shoes at Low Speeds. Journal of Drive and Control, 2015. 12(2): p. 21-26.
16. Michael, P., et al., Hydraulic Fluid Efficiency Studies in Low-Speed High-Torque Motors SAE Technical paper 2009-01-2848. 2009.
17. Michael, P., et al. An Investigation of Hydraulic Fluid Properties and Low-Speed Motor Efficiency. in 7th International Fluid Power Conference. 2010. Aachen, Germany.
18. Michael, P.W., et al., Lubricant Chemistry and Rheology Effects on Hydraulic Motor Starting Efficiency. Tribology Transaction, 2012. 55(5): p. 549-557.
19. ISO 4409:2007, Second edition 2007-04-01, Hydraulic fluid power -- Positive-displacement pumps, motors and integral transmissions -- Methods of testing and presenting basic steady state performance. 2007.
20. ISO, ISO 8426:2008 Hydraulic fluid power -- Positive displacement pumps and motors -- Determination of derived capacity. 2008.
21. Busch, A. and J. Gottschang, Ölbehälter – Optimierungen für die Zukunft. O+P, 2015(1-2).
22. Achten, P. and S. Eggenkamp, Barrel tipping in axial piston pumps and motors. Proc. 15th Scandinavian International Conference on Fluid Power SICFP17, June 7-9, 2017, 2017.
23. Achten, P.A.J., T.L.v.d. Brink, and G.E.M. Vael, A robust hydrostatic thrust bearing for hydrostatic machines. Proc. 7th IFK, March 22-24, 2010, Aachen, Germany, 2010: p. 100-112.

ANNEX A

SIMPLIFIED HYDRAULIC CIRCUIT OF THE LOW SPEED TEST BENCH



1. pump or motor to be tested
2. linear actuator incl position sensor
3. torque meter
4. flow meter case drain flow
5. load valve
6. supply high pressure side
7. supply low pressure side

ANNEX B

SPECIFICATIONS OF THE LOW-SPEED TEST BENCH

test speed	sprocket with 60 teeth		sprocket with 36 teeth	
	n = 0.0084 rpm	n = 0.558 rpm	n = 0.014 rpm	n = 0.93 rpm
rotational speed of the motor	50 rpm	3280 rpm	50 rpm	3280 rpm
transmission ratio of the gear box	50 -	50 -	50 -	50 -
spindl ratio	5 mm/rev	5 mm/rev	5 mm/rev	5 mm/rev
spindl rotational speed	1 rpm	65,6 rpm	1 rpm	65,6 rpm
spindl translational speed	5 mm/min	328 mm/min	5 mm/min	328 mm/min
number of teeth of the sprocket	60 -	60 -	36 -	36 -
rotational speed of the test unit	0,00840 rpm	0,558 rpm	0,0140 rpm	0,931 rpm
duration of 1 revolution	119,05 minutes	1,79 minutes	71,43 minutes	1,07 minutes
stroke length	700 mm	700 mm	700 mm	700 mm
maximum number of revolutions	1,225 -	1,225 -	2,041 -	2,041 -
rotational sensor	16 pulses/rotation	16 pulses/rotation	16 pulses/rotation	16 pulses/rotation
total transmission ratio	5715 -	5715 -	3429 -	3429 -
accuracy rotational position	254 pulses per °	254 pulses per °	152 pulses per °	152 pulses per °
Max. Force	6000 N	6000 N	6000 N	6000 N
Max. torque	500 Nm	500 Nm	327 Nm	327 Nm
Max. motor/pump size @ 500 bar	63 cc	63 cc	41 cc	41 cc

ANNEX C

LIST OF SENSORS AND SENSOR SPECIFICATIONS

Measurement	Sensor	Range	Accuracy	Brand
Torque (stator)	KiTorque 4541A	-	-	Kistler
Torque (rotor)	KiTorque 4550A500	-500...500 Nm	0.05% fso	Kistler
Low pressure level	STJE	0...35 bar	0.05% fso	Honeywell
High pressure level	STJE	0... 520 bar	0.05% fso	Honeywell
Temperature	Type 13 PT100 class B	-50 ... +400 C	±0.3 °C	Testo
Flow leakage	VSI 0.1/16	0.01 ... 10 l/min	± 0.3 %	VSE
Flow high pressure	VS2	0.1 ... 120 l/min	± 0.3 %	VSE